

Non-Newtonian Flow Between Concentric Cylinders Calculated from Thermophysical Properties Obtained from Simulations¹

A. P. Narayan,² J. C. Rainwater,^{3,4} and H. J. M. Hanley^{2,3}

A study of the Weissenberg effect (rod climbing in a stirred system) based on nonequilibrium molecular dynamics (NEMD) is reported. Simulation results from a soft-sphere fluid are used to obtain a self-consistent free-surface profile of the fluid of finite compressibility undergoing Couette flow between concentric cylinders. A numerical procedure is then applied to calculate the height profile for a hypothetical fluid with thermophysical properties of the soft-sphere liquid and of a dense colloidal suspension. The height profile calculated is identified with shear thickening and the forms of the viscometric functions. The maximum climb occurs between the cylinders rather than at the inner cylinder.

KEY WORDS: colloidal suspension; Couette flow; rheology; shear thickening; soft-sphere fluid; Weissenberg effect.

1. INTRODUCTION

In previous work, Rainwater et al. [1, 2] discussed an approach to solve a rheological problem that differed from the traditional. They solved a rheological flow pattern directly, *given* the thermodynamic properties and the viscometric functions of the fluid. In contrast, the conventional approach *infers* the fluid properties after having assumed the equations of motion. The direct approach was feasible because nonequilibrium molecular dynamics (NEMD) can in principle predict the properties for a model liquid under

¹ Paper presented at the Twelfth Symposium on Thermophysical Properties, June 19-24, 1994, Boulder, Colorado, U.S.A.

² Department of Chemical Engineering, University of Colorado, Boulder, Colorado 80309, U.S.A.

³ Thermophysics Division, National Institute of Standards and Technology, Boulder, Colorado 80303, U.S.A.

⁴ Author to whom correspondence should be addressed.

shear. Specifically, Rainwater et al. examined the Weissenberg effect [3], which is the phenomenon observed when a non-Newtonian fluid is sheared between vertical, concentric cylinders. In this paper, we refine the calculations of Refs. 1 and 2 by using density dependences of some viscometric functions that were not previously available and also investigate a possible Weissenberg effect for a colloidal suspension that displays dramatic variations in its viscometric functions.

2. EQUATIONS OF MOTION AND THEIR SOLUTION

The equations of motion are those which describe the behavior of a fluid between vertical, concentric rotating cylinders given [4] cylindrical coordinates (r, θ, z) with their respective unit vectors \hat{e}_r , \hat{e}_θ , and \hat{e}_z , where $z = 0$ is the rest-state free surface of the liquid. We define the radii of the inner and outer cylinders as a and b with angular velocities of rotation Ω and $\lambda\Omega$, respectively; for this calculation $\lambda = 0$.

The assumptions invoked in the problem are, first, that the pressure tensor does not depend on the vorticity or the higher-order velocity gradients, and second, that the results and expressions for planar shear flow carry over to cylindrical shear flow. We will use numerical values of the properties of a model fluid calculated from NEMD in the planar configuration. A detailed derivation for the appropriate equations of motion can be found in Ref. 1, and here we only list the set of coupled nonlinear algebraic and integral equations in terms of the pressure tensor \mathbf{P} and its components P_{ij} , where $(ij) = (r, \theta, z)$, the pressure p , the stream velocity \mathbf{u} , the density ρ , the shear rate $\dot{\gamma}$, the shear viscosity η_+ , and the two coefficients representing the viscometric functions, η_- and η_0 , which represent the normal stresses, $\eta_-(\dot{\gamma}) = -[P_{\theta\theta} - P_{rr}]/2\dot{\gamma}$ and $\eta_0(\dot{\gamma}) = -\{P_{zz} - [\frac{1}{3}(P_{\theta\theta} + P_{rr})]\}/2\dot{\gamma}$ [5]. The equations are

$$\dot{\gamma}(r) = \frac{B}{r^2 \eta_+[\dot{\gamma}(r), \rho(r)]}; \quad B = \text{const} \quad (1)$$

$$u_\theta = \Omega r + r \int_a^r dr' \frac{\dot{\gamma}(r')}{r'} \quad (2)$$

$$P_{rr}(r) = P_{rr}(a) + \int_a^r dr' \left\{ \frac{\rho(r') [u_\theta(r')]^2}{r'} - \frac{2\dot{\gamma}(r') \eta_-[\dot{\gamma}(r'), \rho(r')]}{r'} \right\} \quad (3)$$

$$P_{zz}(r) = P_{rr}(r) - \dot{\gamma}(r) \{ 2\eta_0[\dot{\gamma}(r), \rho(r)] + \eta_-[\dot{\gamma}(r), \rho(r)] \} \quad (4)$$

$$P_{zz}(r) = p[\dot{\gamma}(r), \rho(r)] - \frac{4}{3} \dot{\gamma}(r) \eta_0[\dot{\gamma}(r), \rho(r)] \quad (5)$$

with the no-slip boundary condition at the wall,

$$u_\theta(b) = \Omega b + b \int_a^b dr \frac{\dot{\gamma}(r)}{r} = 0 \tag{6}$$

The position-dependent density is written as

$$\rho(r) = \bar{\rho} + \delta\rho(r) \tag{7}$$

where $\bar{\rho}$ is the average density and $\delta\rho(r)$ is calculated using the condition

$$\int_a^b r dr \delta\rho(r) = \frac{\Delta\rho}{2} (b^2 - a^2) \tag{8}$$

where $\Delta\rho$ is the change in the average density of the fluid as a result of the applied shear. Equation (8) replaces the normalization equation used previously [1], where the total density was constrained to remain at the average density. In the current scheme, an average shear rate is calculated from the shear rate profile, and the density corresponding to this is evaluated given the ρ - $\dot{\gamma}$ relationship from simulation, which in turn is used as an input to the iterative process [6]. The free-surface profile is given by the equation

$$h(r) = \frac{P_{zz}(r) + C}{\rho g} \tag{9}$$

where C is a constant and g is the acceleration due to gravity.

The above equations are solved numerically and iteratively [6]. Initially, the density is set to be constant. We start by guessing at B in Eq. (1), and thus obtain a shear rate profile $\dot{\gamma}(r)$. Since $\eta_+ = \eta_+^{(0)} - \eta_+^{(1)\prime\prime\prime}$, Eq. (1) is a cubic equation in $\dot{\gamma}^{\prime\prime\prime}$ and we solve for $\dot{\gamma}$ by extracting the appropriate root. The calculation of the shear-rate variation also evaluates the fluid velocity at the outer cylinder, which we set equal to zero. We keep varying B until this boundary condition is satisfied. The velocity profile is then integrated to yield the values for the pressure tensor components from Eqs. (3) and (4).

The expression for the pressure tensor from the NEMD simulation also yields a direct expression for P_{zz} , Eq. (5). However, we find initially that the two solutions do not agree. The disagreement arises from our initial imposition of constant density (which, incidentally, implies that the fluid is incompressible). The final solution is then obtained by a series of iterations, where the local density is perturbed using Eq. (7) until the two expressions for the P_{zz} match to within a certain precision. In this calculation, a precision value of 10^{-3} is used.

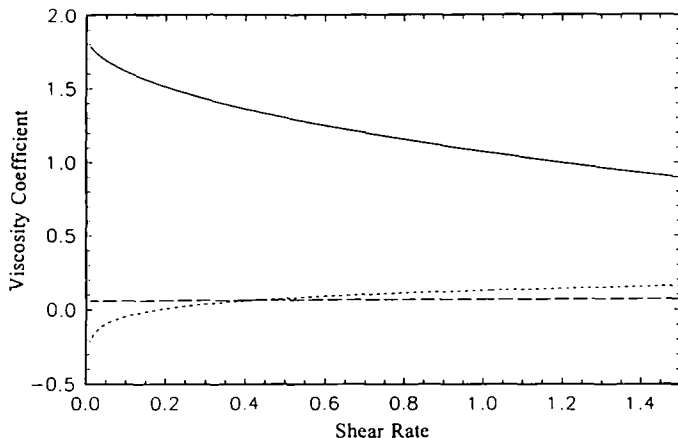


Fig. 1. Variation of the generalized viscosities or viscometric functions η_+ (—), η_- (---), and η_0 (· · ·) as a function of shear rate for the soft-sphere liquid [7].

3. RESULTS FOR THE SOFT-SPHERE FLUID

Our numerical estimate of the free-surface profile for the fluid between rotating cylinders is based on the thermophysical and rheological properties of the soft-sphere fluid reported by Hood et al. [7] from their NEMD study. The variation of these properties as a function of pressure, density, and the shear rate is given in dimensionless form in the appendix to Ref. 7 and is displayed in Fig. 1. To proceed, we have to select numerical values

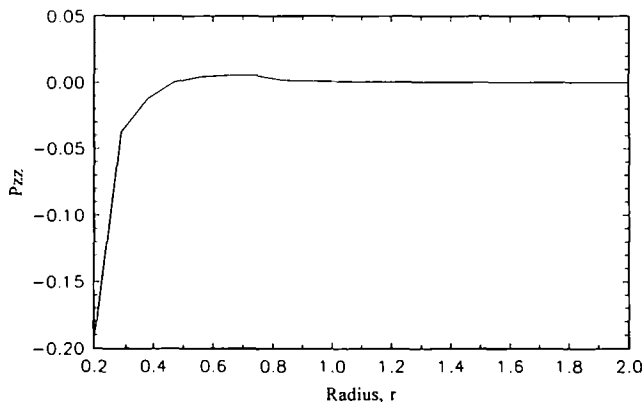


Fig. 2. Plot of the calculated $P_{zz}(r)$, proportional to the free-surface height profile, for the soft-sphere liquid under shear. $P_{zz} = 0$ corresponds to the free surface of the liquid at a state of rest.

for the geometry of the problem. Accordingly, to conform with the previous calculations of Rainwater et al. [1], the radii of the inner and outer cylinders were set at 0.2 and 2.0, and the computation was carried out with $\lambda = 0$ and $\Omega = -0.3$.

The solution gives the height profile shown in Fig. 2. The result is in excellent agreement with the earlier work, though the depth of the depression is larger. The final height profile, which is proportional to $P_{zz}(r)$, is the same—a depression at the inner cylinder and a flattening out as the radius increases and the shear rate falls off, leaving the surface near the outer cylinder virtually in a state of rest.

4. THE WEISSENBERG EFFECT IN A DENSE COLLOIDAL SUSPENSION

We use the calculation of the simple fluid as the basis for the second objective of this paper: namely, to predict a Weissenberg effect for a dense colloidal suspension. Laun [8] has investigated the behavior of a dense colloidal suspension of 322 nm-diameter charged latex spheres in glycol at a volume fraction of 0.51. The fluid has interesting properties. It displays shear thinning at low shears and has a steep shear-thickening regime at higher shears as shown in Fig. 3. Figure 3 plots the shear viscosity versus the shear stress τ , where $\tau = \eta + \dot{\gamma}$. Such behavior is not unusual, but it was observed that the normal pressure differences satisfied the relations $N_1 = -\eta + \dot{\gamma}$ and $N_2 = -N_1/2$, where N_1 and N_2 represent the first and second normal stresses, for a shear $\dot{\gamma} > 10 \text{ s}^{-1}$.

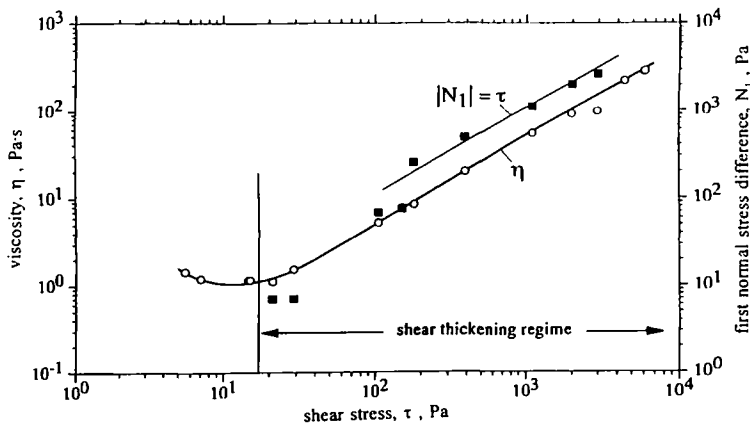


Fig. 3. Plot of the shear viscosity η , and the normal stress N_1 as experimentally determined by Laun [8] for a colloidal suspension.

Hence, in our notation,

$$\eta_0 = 0 \quad (10)$$

and

$$\eta_{\pm} = -\frac{\eta_{\pm}}{2} \quad (11)$$

The free-surface height profile was computed by means of the procedure described. Our fluid is a hypothetical composite that obeys the Laun viscometric functions for $\dot{\gamma} > 10 \text{ s}^{-1}$, but has the properties of the soft-sphere liquid when subjected to a lower shear rate. In order to merge smoothly the shear-viscosity function $\eta_{\pm}(\dot{\gamma})$ over the whole $\dot{\gamma}$ range, we constructed dimensionless curves, $\eta_{\pm}(\dot{\gamma})/\eta_{\pm}(0)$ vs. $t\dot{\gamma}$, where $\eta_{\pm}(0)$ is the viscosity at zero shear, for both fluids. The unscaled shear viscosity for the Laun fluid obeys the relationship $\eta_{+} = 2.13796\dot{\gamma}^{-0.67} \text{ Pa}\cdot\text{s}$ in the shear-thinning regime and $\eta_{+} = 1.269 \times 10^{-18}\dot{\gamma}^{13.8435} \text{ Pa}\cdot\text{s}$ in the shear-thickening regime. The parameter t is a relaxation time. A proper choice for t for the Laun viscosities merges the two data sets. We choose $t = 10 \text{ s}$ for the Laun data [6], and we have a dimensionless $t = 1$ for the soft sphere. Given a scaled shear viscosity and a scaled shear rate, the viscometric functions follow from Eqs. (10) and (11). We further assume that the density dependences of the viscosities are those of the soft sphere. We also assume the pressure dependence on the shear rate given for the soft-sphere fluid extrapolates into the shear-thickening regime.

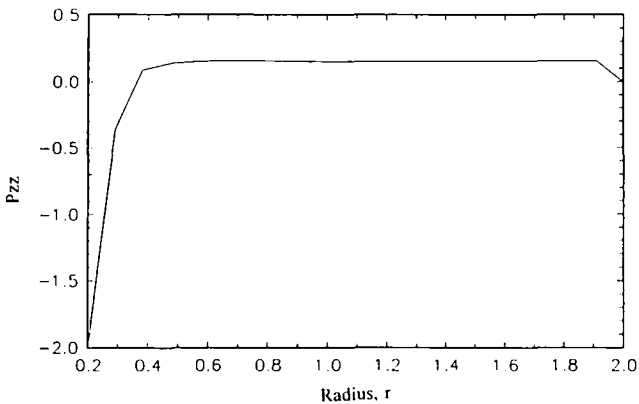


Fig. 4. Plot of the calculated $P_{zz}(r)$, proportional to the free-surface height profile, for the hypothetical fluid composed of the soft-sphere fluid and the colloidal suspension of Laun. Note the appearance of a bulge.

The predicted free-surface profile for our hypothetical fluid is shown in Fig. 4. The profile is a "bulge" and shows a depression at the inner cylinder, a relatively flat profile above the rest-state surface, and a sharp drop near the wall. While such a profile is not excluded by the general theory of the Weissenberg effect [4] and resembles one that was observed experimentally by Beavers and Joseph [9] in a polymer melt, it is unusual. We therefore conclude this paper by speculating why it has this particular form.

The numerical values of the input parameters required by the equations of motion are altered systematically and the subsequent height profile is calculated. Details can be found in Ref. 5, and we only list the main conclusion here. Let us consider a critical shear rate $\dot{\gamma}_c$ above which the fluid obeys the Laun relations and displays shear thickening with respect to the shear imposed on the liquid. We find that climbing occurs only when the maximum shear rate sustained in the liquid is greater than or equal to $\dot{\gamma}_c$. Altering the shear-rate profile or arbitrarily adjusting the $\dot{\gamma}_c$ causes the climbing effect to become more or less pronounced, depending on the degree of overlap. If a shear of $\dot{\gamma}_c$ is never reached in the rotating fluid, the profile reverts to that observed in the simple fluid, which is to be expected.

Sample calculations [6] show that if we include the normal pressure differences of Laun in the calculation but exclude the fact that the fluid is shear thickening, we obtain a rod-climbing Weissenberg effect. Hence, it appears that the combination of the behavior of the Laun normal pressure differences with shear thickening is responsible for the bulge.

ACKNOWLEDGMENT

This work was supported in part by the U.S. Department of Energy, Office of Basic Energy Sciences, Division of Chemical Science.

REFERENCES

1. J. C. Rainwater, H. J. M. Hanley, T. Paszkiewicz, and Z. Petru, *J. Chem. Phys.* **83**:339 (1985).
2. J. C. Rainwater and H. J. M. Hanley, *Int. J. Thermophys.* **6**:595 (1985).
3. K. Weissenberg, *Nature* **159**:310 (1947).
4. D. D. Joseph and R. L. Fosdick, *Arch. Rat. Mech. Anal.* **49**:321 (1973).
5. S. Hess, *Physica A* **118**:79 (1983).
6. A. P. Narayan, The Weissenberg effect in simple dense liquids, Master's thesis, University of Colorado, May 1994.
7. L. M. Hood, D. J. Evans, and H. J. M. Hanley, *J. Stat. Phys.* **57**:729 (1989).
8. H. M. Laun, personal communication (BASF Aktiengesellschaft, Ludwigshafen, Germany) (1993).
9. G. S. Beavers and D. D. Joseph, *J. Non-Newtonian Fluid Mech.* **5**:323 (1979).